Journal of Nano- and Electronic Physics
Vol. **16** No 3, 03018(6pp) (2024)

Журнал нано- та електронної фізики
Том **16** № 3, 03018(6cc) (2024)

OPEN ACCESS

REGULAR ARTICLE

Visible light- Driven Cesium-Titanium Iodide (Cs_2TiI_6) Double Perovskite Photocatalytic dye Degradation

Sujubili Narzary[1], Sanat Das[1], Kunal Chakraborty[1], Mahua Gupta Choudhury[2], Samrat Paul[1,*]

[1] *Advanced Materials Research and Energy Application Laboratory (AMREAL), Department of Energy Engineering, North-Eastern Hill University, Shillong-793022, India*
[2] *Department of Animal Health and Fisheries Sciences, Indian Council for Agricultural Research, North Eastern Hill Region Research Centre (NEHRC), Umiam, Shillong-793103, India*

(Received 15 April 2024; revised manuscript received 20 June 2024; published online 28 June 2024)

Developing novel photocatalytic materials for removing organic contaminants has been a research focus. The current study reports the synthesis of third-generation photocatalysts perovskites and their photocatalytic efficacy. The lead-free cesium-based titanium halide Cs_2TiI_6 double perovskite was successfully synthesized via the solution processing method and characterized by various spectroscopic and morphological characterization techniques such as X-ray diffraction (XRD), UV-visible spectroscopy, Zeta potential, and Transmission Electron Microscope (TEM). The novel aspect of this study is to investigate the photocatalytic efficacy of the Cs_2TiI_6 double perovskite.Various morphology and spectroscopy characterization insights about synthesized photocatalysts were explored. Eosin Y (EY) and Eosin B (EB) were chosen as the model compounds for degradation in this work due to their wide applications in industry. The photocatalytic degradation efficiency of Eosin Y and Eosin B dye by Cs_2TiI_6 perovskite photocatalysts after exposure of 240 minutes to visible light was 85.08% and 13.66% respectively. The rate constant of degradation of Eosin Y is approximately 14.66 times larger than that of Eosin B.

Keywords: Cesium titanium iodide, Lead-free, Photocatalysis, Dye degradation, Eosin.

DOI: 10.21272/jnep.16(3).03018 PACS numbers: 77.84.Bw, 82.45.Jn

1. INTRODUCTION

Water contamination is a major global issue affecting human life and natural ecosystems [1]. The unprecedented rise in the human population and the expansion of industry have caused the quality of water to decline, adversely affecting all living things, including humans[2]. Therefore, to reduce the impact on the environment and public health, it is crucial to ensure that industrial wastewaters are properly treated before disposal into the water bodies [2, 3]. The most prevalent contaminants in water are organic dyes and pigments, found in various industrial effluents, including leather, textiles, paper, printing, and cosmetics industries [2]. Eosin Y and Eosin B are two closely related compounds. Eosins are a type of red fluorescent dye [4, 5].Wastewater containing these dyes causes serious environmental issues due to its stability, high toxicity, poor biodegradability, and dark color [6]. These hazardous organic pollutants can be removed from wastewater by using Advanced Oxidation Processes (AOPs), which convert them into carbon dioxide and water. AOPs offer a promising solution for mineralizing bio-resistant organic contaminants in wastewater [3]. In the list of different degradation techniques, semiconductor photocatalysis has drawn a lot of interest as an environmentally acceptable technique for hydrogen production (H_2), degradation of organic dyes, carbon dioxide reduction, and antibacterial activity [3, 7].

In the past few decades, more researchers have concentrated on the creation of new-generation photocatalytic materials due to the growing awareness of the removal of organic impurities using photocatalytic technological advances.Metal halide perovskites (MHPs) have been gaining popularity in photocatalysis due to their impressive optoelectronic properties, including optimum band structures, long charge carrier lifetimes, high carrier mobility, high photoluminescence quantum yields, and high absorption coefficient [8]. Halide perovskites have excellent optoelectronic features that make them suitable for a wide range of applications such as light-emitting diodes, solar cells, field effect transistors, photodetectors, lasers, thermoelectrics, α-particle detection, X-ray detection, etc [9]. In one study, a $Cs_2AgBiCl_6$-based photocatalyst was fabricated and it was able to degrade Sudan III dye 95 % in 10 minutes under exposure to visible light irradiation [10]. Wu *et al.* reported that lead-free double perovskites $Cs_2AgBiBr_6$synthesized via a facile hot-injection method for photocatalytic nitric oxide (NO) removal could reach an exciting removal rate of 97 % [11]. Recently, the simulation of $Cs_2AgBiBr_4$-based solar cells has been studied using SCAPS-1D, giving 86.09 % quantum efficiency [12]. Currently, most of the research

* Correspondence e-mail: paulsamrat17@gmail.com

Cite this article as: S. Narzary et al., *J. Nano- Electron. Phys.* 16 No 3, 03018 (2024) https://doi.org/10.21272/jnep.16(3).03018

based on Cs_2TiX_6 (X = Cl, Br, I, F) has been undertaken on solar cells.Chen *et al.* report on Cs_2TiBr_6-based perovskite solar cells in which Cs_2TiBr_6 thin films exhibit a consistent efficiency of up to 3.3 % [13]. There is a very limited number of studies on Cs_2TiI_6-based optoelectronic applications, and the majority of the research lacks continuity with practical data. A novel lead-free Cs_2TiI_6 double perovskite material for solar cells and α-particle detection is examined using drift-diffusion theory, first-principles calculations, and the Monte Carlo method. The study reveals that Cs_2TiI_6 shows significant potential in photovoltaic cells and radiation detection [9].

In this article, the authors proposed a novel non-toxic perovskite photocatalyst Cs_2TiI_6 for photocatalytic dye degradation. The main objectives of this study are to fabricate Cs_2TiI_6 using a solution processing method and evaluate the photocatalytic dye degradation of Cs_2TiI_6 under visible light irradiation.

2. MATERIALS AND METHODS

2.1 Materials

All the chemical reagents were of analytical quality and used without further purification. The chemical reagents used to synthesize Cs_2TiI_6 were Cesium iodide (99.9 %), Titanium (IV) iodide, and HI. All the chemicals were purchased from Sigma-Aldrich and Merck (India). All the aqueous solutions were prepared with double-distilled water.

2.2 Synthesis

Cs_2TiI_6 solution was synthesized using the solution processing method with the following chemical reaction

$$2CsI + TiI_4 \rightarrow Cs_2TiI_6 \quad (1)$$

A hydroiodic acid (HI) was combined with a Cesium iodide (CsI). The transparent solution quickly changed into a brownish-black solution made of Cs_2TiI_6 after adding a sufficient quantity of titanium iodide (TiI_4) liquid to the combined solution [14]. The solid-liquid mixture is then centrifuged and the extra liquid is discarded.The resulting blackish-brown powder is oven-dried at 80 °C to remove the remaining solvent and excess TiI_4, without exposing the Cs_2TiI_6 powder to an ambient atmosphere. The dry powder is annealed in the muffle furnace at 100 °C for 30 minutes to improve the crystallinity of the prepared sample [15].

2.3 Characterization

The perovskite photocatalyst synthesized by the solution processing method was characterized by various spectroscopical and morphological characterization techniques such as X-ray diffraction (XRD), UV-visible spectroscopy, Zeta potential, and Transmission Electron Microscope (TEM). XRD analysis (XRD, D8 Advance Bruker, Germany) was examined to identify the phase structure and crystalline size of the powder samples. UV-vis diffuse absorbance spectra were measured using a UV-vis spectrometer (Lambda 650 Perkin Elmer Spectrometer) equipped with an integrating sphere attachment. The Zeta potential of the prepared perovskites has been measured using dynamic light scattering (Litesizer 500, Anton Paar). The TEM model JEM-100CX II, JEOL Japan was used for analyzing the topography and surface morphology of the samples.

2.4 Photocatalysis

The synthesized photocatalysts were studied for their potential to degrade some of the organic dyes namely, Eosin B and Eosin Y. The photocatalytic activity was conducted under a 200 W Xenon lamp using visible light of illuminance of 940 lux as a light source. For every reaction, 0.01 g catalyst in 100 mL dye solution of 25 ppm was used. To attain adsorption/desorption equilibrium the reaction was kept in a dark condition for 15 minutes. Then the solution was exposed to the light for 4 hours. During the decomposition process at every 30-minute interval, a 3-5 mL sample was drawn for absorbance measurement and centrifuged to remove the catalyst. Thereafter, the centrifuged clear solution was analyzed using a UV-vis spectrophotometer (SL 210 - ELICO) to measure the extent of dye degradation.

3. RESULTS AND DISCUSSION

3.1 X-ray Diffraction

The XRD (X-ray diffraction) pattern of Cs_2TiI_6 is shown in Fig. 1. Powder X-ray diffraction measurements can determine unit cell characteristics of the materials. The XRD pattern of as-prepared Cs_2TiI_6 is consistent with the corresponding literature [14]. The formation of Cs_2TiI_6 is confirmed as it exhibits 2θ peaks at 27.31°, 30.16°, 38.77°, 44.01°, 50.04°, 52.09°, 55.38°, and 64.20° corresponds to *hkl* planes at (222), (400), (422), (440), (620), (622), (444) and (800) respectively [14, 16].

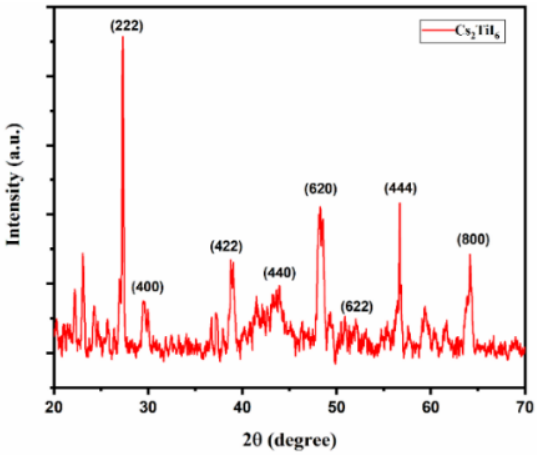

Fig. 1 – Powder XRD pattern of Cs_2TiI_6

A successful synthesis is confirmed by the good agreement between the previously reported values and measured data. the presence of additional peaks indicates the unreacted residues of CsI.The crystallite size of the intense peak of the synthesized material Cs_2TiI_6 is calculated from the broadening XRD peak (222) using the Debye Scherrer equation, (Eq. 2).

$$D = \frac{K\lambda}{\beta \cos\theta} \quad (2)$$

where D is the crystallite size, β is the full-width half

maximum (FWHM) of the most intense peak, θ is the diffraction angle, λ is the wavelength of X-ray radiationand K is the shape factor. The crystallite size of the Cs_2TiI_6, calculated by using the Debye Scherrer equation is 52.25 nm. By using Bragg's law, the d-spacing of the respective diffraction angle was determined i.e. $\lambda = 2d\sin\theta$, where λ is the X-ray radiation wavelength, θ is the diffraction angle and d is the interplanar spacing between the lattice planes. The calculated interplanar spacing of the respective diffraction angle of the (222) plane is 0.33 nm. The results show that Cs_2TiI_6 exhibits a cubic crystal structure with lattice parameters of 11.43 Å [14, 16].

3.2 3.2. UV-visible Spectrophotometer

The UV-vis diffuse reflectance spectrum was studied to examine the spectral response of the prepared sample. The absorbance spectrum of Cs_2TiI_6 in the wavelength range of 200-800 nm is shown in Fig. 2(a). The absorbance spectrum revealed that Cs_2TiI_6 has wide peaks between 500 nm and 700 nm, which indicates its suitability for optoelectronic applications.The Cs_2TiI_6 exhibitsabsorption in the near-IR region [14]. The bandgap energy of Cs_2TiI_6 was derived from the Tauc plot of the transformed Kubelka-Munk function of UV-visible spectroscopic absorbance spectrausing the expression $(\alpha h\nu)^2 = A(h\nu - E_g)$; where h is Planck constant, α is absorption coefficient, ν is the frequency, A is the proportionality constant and E_g is the band gap. The Tauc plot of the Cs_2TiI_6 is shown in Fig. 2 (b).

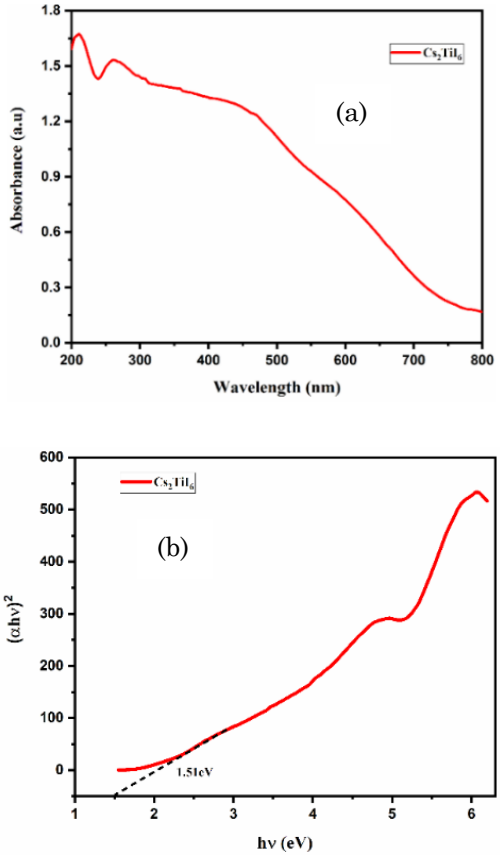

Fig. 2 – (a) UV-visible spectroscopy absorbance spectra of Cs_2TiI_6 (b) Corresponding Tauc plot

3.3 Zeta Potential

Zeta potential is analyzed to calculate the surface charge of the materials in a colloidal solution. It measures the stability of the samples against agglomeration. In this experiment,ethanol was used as a solvent for zeta potential analysis. The zeta potential analysis spectrum of Cs_2TiI_6 is shown in Fig. 3. The zeta potential values ranging between – 10 mV and + 10 mV are regarded as approximately neutral while highly stable nanoparticles range from greater than +30 mV to less than – 30 mV [17].The zeta potential adjacent to zero promotes agglomeration. The mean zeta potential value of Cs_2TiI_6 is 30.8 mV. The positive charge on nanoparticles enhances the interaction with anionic dye. Compared to the other metal halide perovskites Cs_2TiX_6 (X=Cl, Br), Cs_2TiI_6 exhibits better stability.

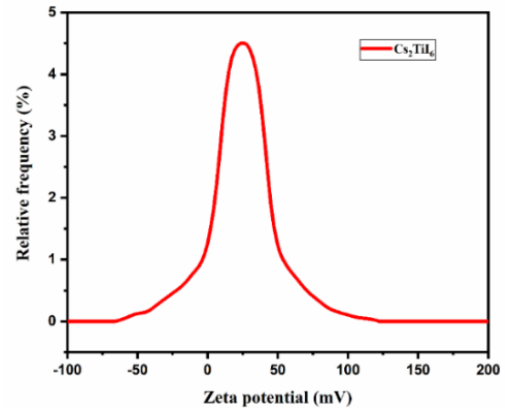

Fig. 3 – Zeta potential analysis spectra of Cs_2TiI_6

3.4 Transmission Electron Microscope (TEM)

The TEM image shows the surface morphology and topography of the Cs_2TiI_6perovskite nanoparticle. Fig. 4 (a) shows the TEM image of Cs_2TiI_6. The HR TEM image shown in Fig. 4 (b) shows the interplanar spacing

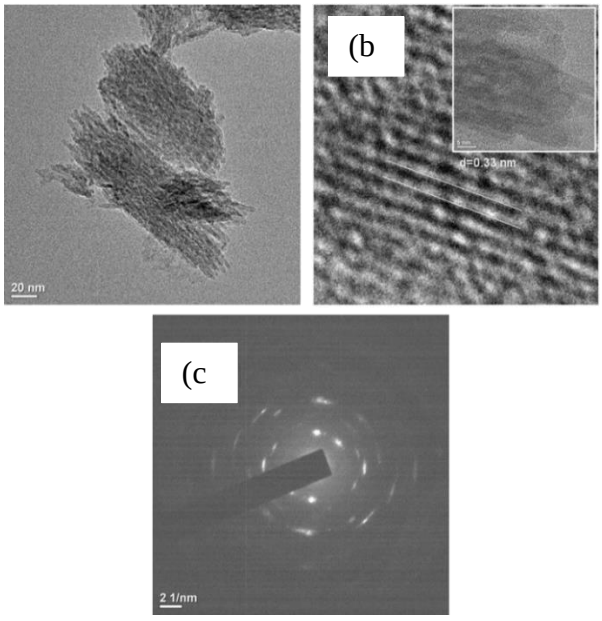

Fig. 4 – (a) LR-TEM image of Cs_2TiI_6, (b) HR-TEM image of Cs_2TiI_6, (c) SAED pattern of Cs_2TiI_6

between two lattice planes. The d-spacing of the nanoparticle calculated from the HR TEM image is found to be 0.33 nm for the (222) plane respectively. The selected area electron diffraction (SAED) pattern of the Cs_2TiI_6 is shown in Fig. 4 (c). The polycrystalline nature of the nanoparticle is seen from the bright diffraction spot of the SAED pattern. The orientation acquired from the TEM image is analogous to the XRD data.

4. PHOTOCATALYTIC PERFORMANCE OF ORGANIC DYES

4.1 Photocatalytic degradation of Eosin Y

The photocatalytic performance of the prepared sample degrading an anionic dye Eosin Y under visible light is shown in Fig. 5. The UV-visible absorbance spectra of the Eosin Y solution photocatalyzed by Cs_2TiI_6 are plotted in Fig. 5 (a). The rate of degradation of Eosin Y by Cs_2TiI_6 is plotted in Figure 5 (b).

The photocatalytic degradation efficiency was calculated by using the following formula,

$$\eta(\%) = \frac{C0-Ct}{C0} \times 100 \quad (3)$$

Where C_0 is the initial concentration of dye and C_t is the-concentration of dye after light irradiation at time t. The rate constants of each reaction were calculated by plotting $-\ln C/C_0$ vs. time (Figure 5 (c)). This analysis shows that the photocatalytic activity of the prepared photocatalyst obeys the first-order reaction kinetics equation $-\ln(C/C_0) = kt$, where k is the rate constant of the photocatalytic reaction. The photocatalytic degradation efficiency of Cs_2TiI_6 perovskite photocatalysts is 85.08 % for Eosin Y.The reaction rate constant of photocatalytic EY degradation of Cs_2TiI_6 is shown in Table 1.

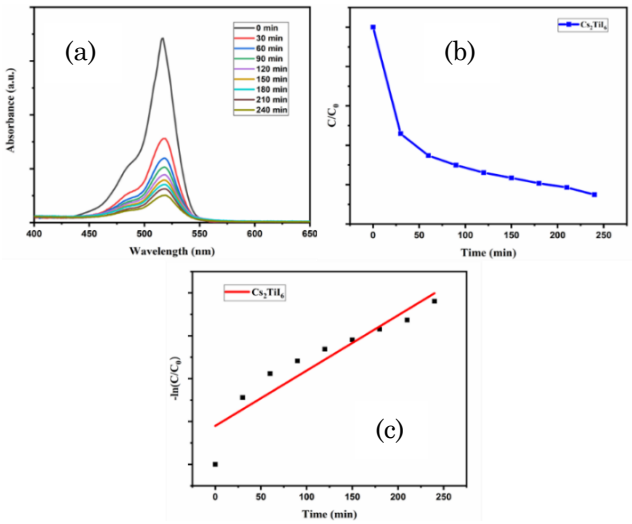

Fig. 5 – Photocatalytic degradation of Eosin Y, (a) UV-visible absorbance spectrum of Cs_2TiI_6, (b) Degradation of Eosin Y with time, and (c) Pseudo first-order kinetics curve

4.2 Photocatalytic Degradation of Eosin B

The photocatalytic performance of the prepared sample degrading Eosin B dye under visible light is shown in Fig. 6. The UV-visible absorbance spectra of the Eosin B solution photocatalyzed by Cs_2TiI_6 are plotted in Fig. 6 (a).

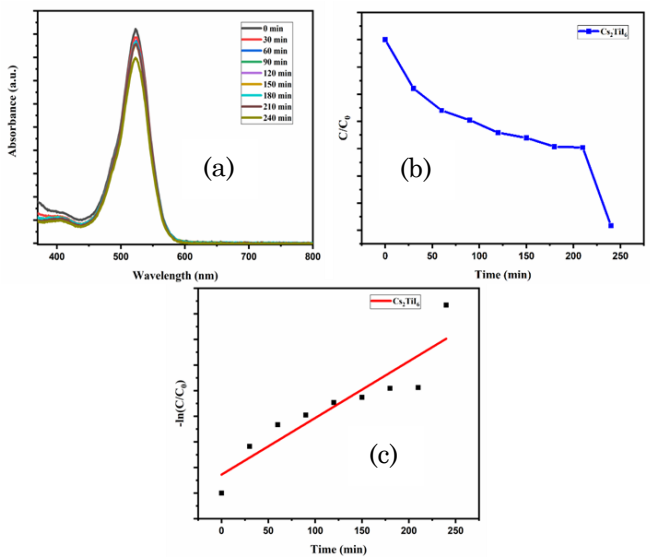

Fig. 6 – Photocatalytic degradation of Eosin B, (a) UV-visible absorbance spectrum of Cs_2TiI_6, (b) Degradation of Eosin B with time, and (d) Pseudo first-order kinetics curve

The rate of degradation of Eosin B by Cs_2TiI_6 is plotted in Figure 6 (b).

From the absorbance spectrum, it has been observed that the degradation of EB is much less as compared to the degradation of EY. The photocatalytic degradation efficiency of Cs_2TiI_6 perovskite photocatalysts is 13.66 % for Eosin B. The rate constant of degradation of EY is approximately 14.66 times larger than that of EB. The reaction rate constant of photocatalytic EB degradation of Cs_2TiI_6 is shown in Table 1.

Cesium-based double perovskite materials have performed well in numerous studies and developments in the realm of photocatalytic applications, such as fuel production and pollution remediation. As summarized in Table 2 these materials are suitable for photocatalytic pollutant degradation.

Table 1 – The reaction rate constant of photocatalytic degradation of Cs_2TiI_6

S. No	Name of Sample	Eosin B k min^{-1} $\times 10^{-3}$	Eosin Y k min^{-1} $\times 10^{-3}$
1.	Cs_2TiI_6	0.4 ± 0.00007	6.45 ± 0.0009

Table 2 – Comparison of reported Cesium-based Photocatalytic pollutant degradation efficiency with present work

Name of perovskites	Light Source	Photocatalytic degradation	Efficiency (%)	Reaction Time (min)
($Cs_2Ag_xNa_{1-x}InCl_6$) Incorporated with Na [18]	Visible Light	Rhodamine 6G & Methyl Orange	94.94 90.39	60 150
$Cs_2AgBiCl_6$ [10]	Visible Light	Sudan III	95.70	10

$Cs_2AgBiBr_6$ [11]	Visible Light	Nitric oxide (NO)	97	N/A
Cs_2TiCl_6 [19]	200 W Xenon Lamp	Eosin B (EB) & Eosin Y (EY)	59.12(EB) 72.35(EY)	240
Cs_2TiBr_6 [19]	200 W Xenon Lamp	Eosin B (EB) & Eosin Y (EY)	48.77(EB) 89.94(EY)	240
Cs_2TiI_6*	200 W Xenon Lamp	Eosin B (EB) & Eosin Y (EY)	13.66(EB) 85.08(EY)	240

*The result corresponds to the presented work

4.3 Mechanism of Photocatalytic Degradation

Halide perovskite materials provide various distinct properties in photocatalysis. The Valence Band Maximum (VBM) and Conduction Band Minimum (CBM) sites are almost optimal for thermodynamically driving diverse photocatalytic reactions. Second, the tuning of chemical composition can easily change band topologies and charge migration characteristics. Finally, ferroelectric and piezoelectric phenomena may enhance photocatalytic activity [8]. The efficiency of a photocatalytic reaction is determined by the potency of the three processes listed below: (i) photon absorption to generate electron and hole pairs, (ii) charge separation and migration to reaction sites on the photocatalyst surface, and (iii) chemical reactions at the photocatalyst surface by the photogenerated electrons and holes [8, 20]. The reaction mechanism of the synthesized perovskite photocatalyst is shown in Fig. 7.

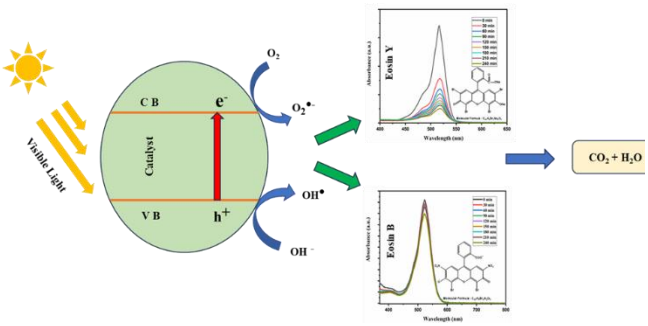

Fig. 7 – Reaction mechanism of photocatalytic degradation

Under exposure to visible light irradiation, the Cs_2TiI_6 metal halide perovskites can absorb photons, and the photogenerated electrons are excited from the valence band (VB) to the conduction band (CB), leaving gaps behind in the VB.Thereafter, the excited holes and electrons undergo a redox reaction with the other molecules. The photogenerated e^- and h^+ reacts with O_2 and OH^- producing $^{\cdot}O_2^-$ and $^{\cdot}OH$ radicals. Finally, the Eosin Y and Eosin B molecules were oxidized into inorganic or nontoxic products of water and carbon dioxide molecules [19].

5. CONCLUSION

In this work, a novel non-toxic perovskite photocatalyst Cs_2TiI_6 for photocatalytic dye degradation was synthesized successfully using a solution processing approach and characterized by various spectroscopical andmorphological characterization techniques. The crystallite size and the interplanar spacingvalue of theCs_2TiI_6, calculated from XRD data is 52.25 nm and 0.33 nm for the lattice plane (222). Additionally, the XRD result shows that Cs_2TiI_6 exhibits a cubic crystal structure with lattice parameters of 11.43 Å. The XRD pattern of as-prepared Cs_2TiI_6 is consistent with the corresponding literature. The bandgap calculated by Tauc plot from a wide peak between 500 nm and 700 nm indicates its suitability for optoelectronic applications. The positive mean zeta value of the Cs_2TiI_6 photocatalyst may enhance the interaction with anionic dye. The polycrystalline nature of the nanoparticle is seen from the bright diffraction spot of the SAED pattern. The orientation acquired from the TEM image is analogous to the XRD data. The photocatalytic degradation efficiency of Eosin Y and Eosin B dye by Cs_2TiI_6 perovskite photocatalysts after exposure of 240 minutes to visible light was 85.08 % and 13.66 % respectively.The rate constant of degradation of Eosin Y is approximately 14.66 times larger than that of Eosin B. Cs_2TiI_6 is a promising next-generation optoelectronic material due to its biocompatibility, environmental sustainability, and versatility in various applications. More research is being done to enhance the photocatalytic efficacy of this material.

ACKNOWLEDGEMENTS

The authors acknowledge SERB, DST, New Delhi (File no-EMR/2016/002430) for the financial support to carry out this work. The authors are also grateful for the support by the Ministry of Tribal Affairs for the NFST Fellowship (Award No 202021-NFST-ASS-01982). The authors gratefully acknowledge the Sophisticated Analytical Instrument Facility (SAIF) of North Eastern Hill University for help with characterization, and the Institute of Advanced Study in Science and Technology for XRD analysis.

REFERENCES

1. S. Li, Q. Lin, X. Liu, L. Yang, J. Ding, F. Dong, Y. Li, M. Irfan, P. Zhang, *RSC Adv.* **8**, 20277 (2018).
2. A. Salama, et al, *Appl. Nanosci.* **8**, 155 (2018).
3. S.G. Poulopoulos, A. Yerkinova, G. Ulykbanova, V.J. Inglezakis, *PLoS One* **14**, 0216745 (2019).
4. A. Hossain, et al., *Am. J. Anal. Chem.* **7**, 863 (2016).
5. E.S. Agorku, et al., *Sustain. Environ.* **9**, 2266632 (2023).
6. M.H. Magar, et al., *Res. Chem.* **4**, 100537 (2022).
7. S. Narzary, K. Alamelu, V. Raja, B.M. Jaffar Ali, *J. Environ. Chem. Eng.* **8**, 104373 (2020).
8. R. Mishra, et al., *Appl. Surf. Sci. Adv.* **9**, 100241 (2022).
9. P. Zhao, et al., *Nano. Res.* **15**, 2697 (2022).
10. K. Guo, et al., *Chemistry – A Eur. J.* **29**, e202300400 (2023).
11. D. Wu, et al., *J. Catal.* **397**, 27 (2021).
12. S. Das, et al., *J. Nano- Electron. Phys.* **16** No 1, 01014 (2024).
13. M. Chen, et al., *Joule* **2**, 558 (2018).

14. S. Aslam, S.A.M. Samsuri, *IOP Conf. Ser. Earth Environ. Sci.* **1281**, 12029 (2023).
15. J. Euvrard, X. Wang, T. Li, Y. Yan, D. B. Mitzi, *J. Mater. Chem. A* **8**, 4049 (2020).
16. C. Kupfer, et al., *Crystal Res. Technol.* **58**, 2200150 (2023).
17. N. Kumari, et al., *Sol. Energy Mat. Sol. C.* **208**, 110408 (2020).
18. J. Sun, Z. Yang, L. Li, Y. Zhang, G. Zou, *Environ. Sci. Pollut. Res.* **28**, 50813 (2021).
19. S. Narzary, S. Das, P.P. Gohain, K. Chakraborty, M.G. Choudhury, S. Paul, *Nanomat. Energy* **13**, 1 (2024).
20. H. Huang, et al., *ACS Energy Lett.* **5**, 1107 (2020).

Цезій-титан йодид (Cs_2TiI_6) видимого світла: подвійна деградація перовскітного фотокаталітичного барвника

Sujubili Narzary[1], Sanat Das[1], Kunal Chakraborty[1], Mahua Gupta Choudhury[2], Samrat Paul[1]

[1] *Advanced Materials Research and Energy Application Laboratory (AMREAL), Department of Energy Engineering, North-Eastern Hill University, Shillong-793022, India*
[2] *Department of Animal Health and Fisheries Sciences, Indian Council for Agricultural Research, North Eastern Hill Region Research Centre (NEHRC), Umiam, Shillong-793103, India*

Розробка нових фотокаталітичних матеріалів для видалення органічних забруднень була фокусом досліджень. Поточне дослідження повідомляє про синтез фотокаталізаторів третього покоління перовскітів та їх фотокаталітичну ефективність. Подвійний перовскіт титану без свинцю на основі цезію Cs_2TiI_6 був успішно синтезований за допомогою методу обробки розчину та охарактеризований різними методами спектроскопічної та морфологічної характеристики, такими як дифракція рентгенівських променів (XRD), УФ-видима спектроскопія, дзета-потенціал та пропускання електронів. Мікроскоп (ПЕМ). Новим аспектом цього дослідження є дослідження фотокаталітичної ефективності подвійного перовскіту Cs_2TiI_6. У роботі досліджені різні морфологічні та спектроскопічні характеристики синтезованих фотокаталізаторів. Eosin Y (EY) і Eosin B (EB) були обрані як модельні сполуки для розкладання в цій роботі через їх широке застосування в промисловості. Ефективність фотокаталітичної деградації барвника перовскітними фотокаталізаторами Cs_2TiI_6 після 240-хвилинної експозиції у видимому світлі становила 85,08 і 13,66% відповідно. Константа швидкості деградації Eosin Y приблизно в 14,66 разів більша, ніж константа Eosin B.

Ключові слова: Йодид титану цезію, Фотокаталіз, Деградація барвника, Еозін.